J Fluoresc (2012) 22:1–7
DOI 10.1007/s10895-011-0951-y

FLUORESCENCE NEWS ARTICLE

Donor-Acceptor Compound Based on Rhodanineacetic Acid-Pyrene Derivative: Red-Light Emitting Fluorescent Organic Nanoparticles

Bo Zhang · Wei Diao · Chun Bi · Jian Sun · Guoxia Han · Yi Shi · Li Sheng · Gui Yin · Lin Pu

Received: 7 June 2011 / Accepted: 7 August 2011 / Published online: 17 August 2011

Abstract A donor-acceptor compound based on Rhodanineacetic acid-pyrene derivative (RAAP), which emits weak yellow-green fluorescence in the methanol solution, was investigated. RAAP nanoparticles with a mean diameter of 50–60 nm were prepared by a simple reprecipitation method without surfactants. The observation of RAAP nanoparticles were undertaken through SEM and TEM method. The emission spectra of RAAP nanoparticles are red-shifted ($\Delta \lambda_{em}$=86 nm) to red region and the intensity is 40-fold higher than that in the methanol solution. Both the J-aggregation and aggregation-induced intramolecular planarization are considered to be the probable mechanism of strong emission for RAAP nanoparticles. The excellent sensibility toward organic vapor which profits from its fluorescence switching behavior is well demonstrated by vapor experiment.

Keywords Donor-acceptor compound · Fluorescent organic nanoparticles · Red-shift · Sensibility · Vapor experiment.

Electronic supplementary material The online version of this article (doi:10.1007/s10895-011-0951-y) contains supplementary material, which is available to authorized users.

B. Zhang · W. Diao · C. Bi · J. Sun · G. Han · G. Yin (✉)
State Key Laboratory of Analytical Chemistry for Life Science, School of Chemistry and Chemical Engineering, Nanjing University, Nanjing 210093, People's Republic of China
e-mail: yingui@nju.edu.cn

Y. Shi · L. Pu (✉)
Key Laboratory of Advanced Photonic and Electronic Materials, Nanjing National Laboratory of Microstructure, School of Electronic Science and Engineering, Nanjing University, Nanjing 210093, People's Republic of China
e-mail: pulin@nju.edu.cn

L. Sheng
Nanjing National Laboratory of Microstructure, School of Physics, Nanjing University, Nanjing 210093, People's Republic of China

Introduction

The research on fluorescent inorganic semiconductor or metal nanoparticles has attracted considerable interest because of their unique properties and multifarious potential applications including photovoltaic cells, light-emitting diodes (LEDs) and so on [1–4]. However, the new topic about fluorescent organic nanoparticles (FONs) has been paid more and more attention due to the diversity and flexibility in materials synthesis and nanoparticle preparation of organic molecules [5]. Nakanishi firstly carried out the systematic research on FONs. They prepared perylene and phthalocyanine nanoparticles by the simple reprecipitation method and demonstrated that this kind of organic nanoparticles could show very different and size-dependent fluorescent properties from those of bulk samples [6–9].

Recently a number of novel donor-acceptor (D-A) type FONs with potential applications in organic light-emitting diodes (OLEDs) have been synthesized and reported [10, 11]. However, the preparation of such organic nanoparticles with remarkable fluorescence efficiency remains a challenging objective, because the strong emission of organic compounds in dilute solution usually becomes rather weak in solid state due to intermolecular vibronic interaction [12–14]. Park and coworks' researches on 1-Cyano-*trans*-1,2-bis-(4′-methylbiphenyl)-ethylene (CN-MBE) particles [12] reported the mechanism of fluorescence enhancement in solid state. They assumed that the fluorescence changes from dilute solution to disperse system of nanoparticles were more or less related to the effects of intramolecular

planarization and a specific aggregation (H- or J-aggregation) in solid state [12, 13]. The pyrene moiety is one of the most effective fluorophores. Most of the compounds using pyrene as fluorophore, which were used as fluorescent chemosensors or dyes [14–24], were reported to emit around 350–550 nm[14–22]. Only a few of them show red-light emission [22, 23].

Herein, we describe a new class of D-A type fluorescent organic nanoparticles (RAAP nanoparticles) with a mean diameter of 50–60 nm, which exhibits strong red-light emission. RAAP was prepared by connecting 1-formylpyrene with rhodanine-3-acetic acid following a modified literature procedure (Scheme 1). Generally, the design principle of this compound is the connection of conjugated structures by rotatable single bond, so that the spectral changes have mainly been attributed to J-aggregation and intramolecular planarization.

Experimental

Reagents, Materials and Equipments

Methanol was of HPLC grade and obtained from Merck. All of the reagents were of analytical grade unless otherwise noted. ^{1}H-NMR and ^{13}C-NMR spectrum were measured using Bruker Ultrashield 300 MHz NMR spectrometer. Chemical shifts were expressed in ppm (in DMSO-d^{6}; TMS as internal standard) and coupling constants (*J*) in Hz. UV–vis spectrum was recorded on Perkin Elmer Lambda 35 spectrophotometer. Fluorescence measurements were performed at room temperature on Perkin Elmer LS-55 spectrophotometer. Mass spectroscopy was recorded with a Thermo LCQ Fleet MS spectrometer in negative ion mode. IR data were measured on a KBr crystal plate, using Bruker VECTOR 22 spectrophotometer. Scanning Electron Microscopy (SEM) images were recorded on a S-4800 electron microscopy at 5.0 kV. Transmission Electron Microscopy (TEM) images were recorded on JEX-200CX transmission electron microscopy. Fluorescence Microscope photos were recorded with an Olympus FV-1000 laser scanning confocal fluorescence microscope. Average particle size was measured by dynamic light scattering (90 plus/BI-MAS).

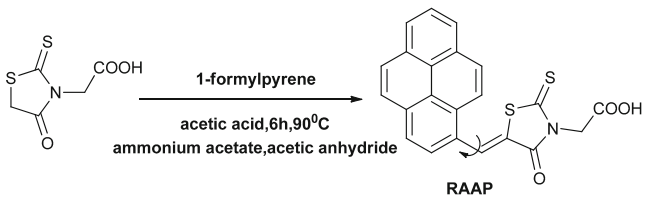

Scheme 1 Synthetic approach for RAAP

Synthesis of RAAP

The compound RAAP was prepared by connecting 1-formylpyrene with rhodanine-3-acetic acid following a literature procedure (Scheme 1) [24].

Preparation of Samples

Preparation of Nanoparticles

The concentrated RAAP solution in methanol (1×10^{-4} M) was diluted with water or water/methanol mixtures. The mixtures were stirred for half an hour and then kept in the darkness before measured. The nanoparticles began to form when water fraction went up. Concentration of RAAP in final water/methanol mixtures was 5×10^{-6} M.

Preparation of Samples for SEM Images

Samples for SEM were prepared by placing few drops of the fluorescent organic nanoparticles (FONs) solution onto a glass cover slip placed on an aluminum stub. The samples were allowed to dry in an oven (45 °C) before viewing under the electron microscope. To enhance contrast and quality of the SEM images, the prepared samples were sputter-coated with gold/palladium.

Preparation of Samples for TEM Images

A drop of nanoparticle solution was deposited on a carbon-coated copper grid, left to dry under high vacuum, and then observation was performed at room temperature at an accelerating voltage of 100 kV.

Preparation of Samples for Fluorescence Microscope Images

A drop of the nanoparticle solution was placed between two slides of glass. The excitation wavelength was set at 505 nm, using suitable filters.

Results and Discussion

RAAP is soluble in common organic solvents such as methanol, methylene dichloride and THF but is insoluble in the water. RAAP nanoparticles were prepared by a simple reprecipitation method without surfactants. According to this method [25–27], water was used as nonsolvent and was gradually added to the RAAP solution in methanol (RAAP concentration 5×10^{-6} M, all tests were undertaken with this concentration). After 76% volume fraction of water was added, RAAP molecules in the mixture solution started to

aggregate into nanosized particles inducing a remarkable fluorescence red-shift from yellow-green to red (Fig. 1, insert). In the case of 90% volume fraction of water addition, solution of the nanoparticles exhibited the most remarkable fluorescence efficiency in the red region. The normalized fluorescence emission spectra of RAAP solution in methanol (isolated state) and RAAP nanoparticles in water/methanol (v/v, 9:1) mixture were investigated in Fig. 1. An obvious red-shift from 542 nm to 628 nm ($\Delta\lambda_{em}$=86 nm) was observed. The excitation spectra of RAAP in isolated state and nanoparticle state obtained at 625 nm show that the emission comes from different chromophores (ESI, Fig. S1).

The Observation of the Shape of RAAP Nanoparticles

The shape of RAAP nanoparticles obtained from water/methanol (v/v, 9:1) mixture was observed by Scanning Electron Microscopy (SEM). SEM image in Fig. 2 shows that RAAP nanoparticles are fine spheres with a mean diameter of 50–60 nm. Figure 3 shows the Fluorescence Microscope image of RAAP nanoparticle solution. A large population of fluorescent dots emitting in the red region can be seen when excited at 505 nm, which confirms the presence of fluorescent organic nanoparticles (FONs) in water/methanol mixtures. The observation by Transmission Electron Microscopy (TEM) leads to the similar result of SEM (Fig. 4). However, SEM and TEM observations are achieved with dried samples. To make sure that nanoparticles are present in the water/methanol mixture, Dynamic Laser Scattering (DLS) experiments were undertaken. The DLS histogram (Fig. 5) shows a normal distribution of RAAP nanoparticles in water/methanol (v/v, 9:1) mixture. The measured diameter is about 60 nm which is consistent with the results recorded by SEM and TEM technique.

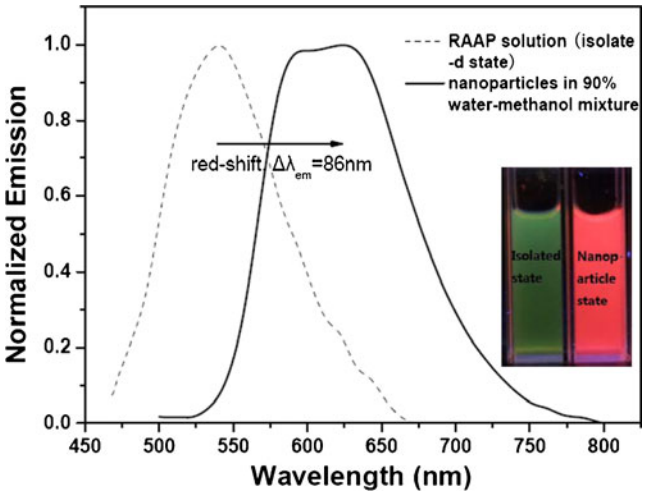

Fig. 1 Normalized fluorescence emission spectra of RAAP solution in methanol (*broken line*) and RAAP nanoparticles in water/methanol (v/v, 9:1) mixture (*solid line*). Insert: photos of RAAP solutions before (*left*) and after (*right*) the formation of nanoparticles under 365 nm irradiation

Fluorescent Property of RAAP Nanoparticles

The fluorescent property of RAAP nanoparticles in the mixed solution of methanol and water with different ratios was investigated as shown in Fig. 6. Upon excitation at 470 nm, RAAP solution (5×10^{-6} M) in methanol emits weak light at 542 nm (yellow-green). With the addition of water, the emission profile is red-shifted to 628 nm (red). This bathochromic effect is depicted in Fig. 3 insert as the plots of the emission maximum shift versus the volume fraction of water%. The enhancement of fluorescence intensity is as well depicted in Fig. 7 as the plots of ratio I/I_0 versus the water fraction (volume%). Quantification of the ratio I/I_0 shows that when the volume fraction of water is increased to 70%, the fluorescence intensity is only 4-fold higher than that in pure methanol solution (I_0). However, the intensity starts to increase rapidly after the addition of 76% volume fraction of water, achieving an intensity maximum at 90% water, which is 40-fold higher than I_0, under identical concentration and measurement conditions. The enhanced emission is clearly depicted by the changes of relative quantum yield (Φ_f) of RAAP (5×10^{-6} M) in water/methanol mictures. Isolated RAAP shows virtually no fluorescence at all (Φ_f=0.004). In the case of 90% fraction of water addition, the Φ_f value of RAAP nanoparticles is 0.180. Fluorescence quantum yields were determined by using rhodamine B in ethanol (Φ_f=0.970) as a refence. Clearly, the emission enhancement is induced by the formation of nanoparticles, or in other words, RAAP is

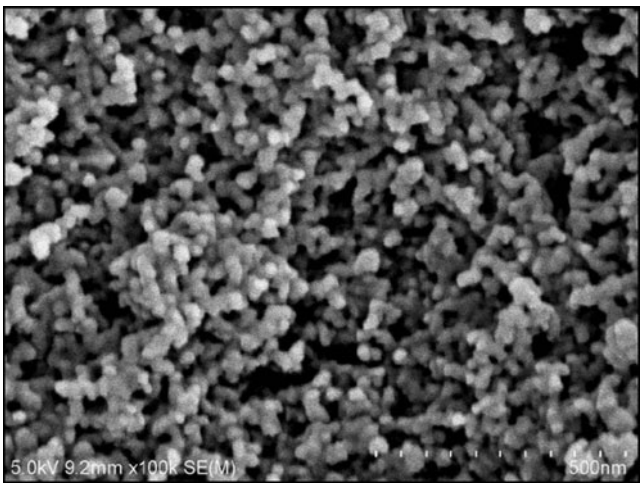

Fig. 2 SEM image of RAAP nanoparticles obtained from water/methanol (v/v, 9:1) mixture

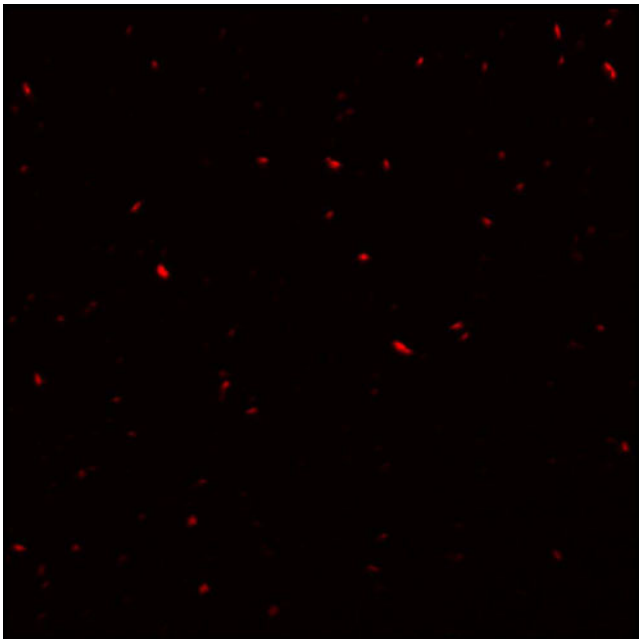

Fig. 3 Fluorescence Microscope image of RAAP nanoparticle solution (water/methanol=9:1, v/v)

AIEE (aggregation induced emission enhancement) active. The distinct red-shift and emission enhancement can be seen by naked eye under 365 nm irradiation (Fig. 1, insert).

Careful analysis of the fluorescence spectra reveals that the emission intensity starts to decrease when the volume fraction of water is increased from 90 to 95% (Fig. S3). The measured intensity at 95% is 35-fold higher than I_0. This emission decrease is attributed to the change in the shape of the aggregates from regular spheres to amorphous ones [26]. When the water ratio is lower than 90%, the RAAP molecules may slowly assemble in an ordered fashion to form more emissive nanoparticles. However, when the water ratio is higher than 90%, the RAAP molecules may quickly cumulate in a random way to form less emissive amorphous powders due to the hydrophobicity of pyrene moiety.

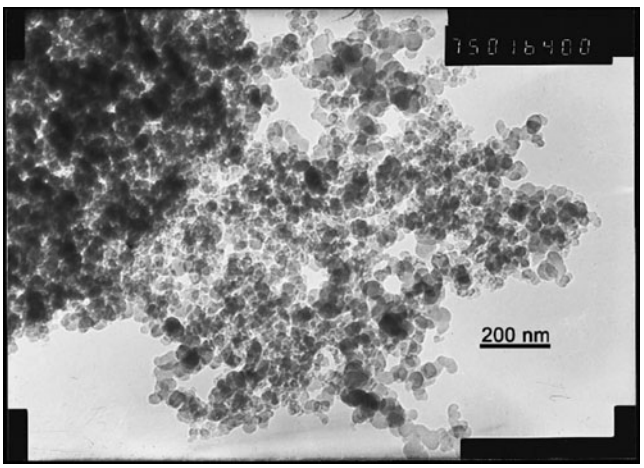

Fig. 4 Transmission Electron Microscopy (TEM) image of RAAP nanoparticles obtained from water/methanol (v/v, 9:1) mixture

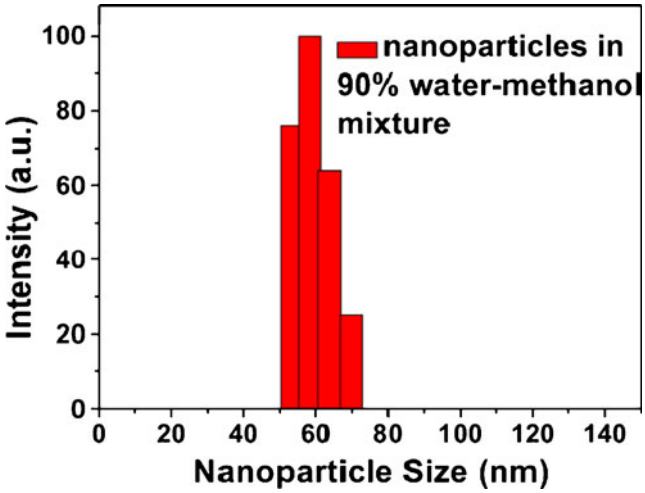

Fig. 5 Size distribution of RAAP nanoparticles in water/methanol (v/v, 9:1) mixture. The finally RAAP concentration is 5×10^{-6} M. The measured diameter of RAAP nanoparticles is about 50–60 nm

RAAP nanoparticles display two excitation bands centered at 505 and 532 nm (Fig. S1), and two emission bands centered at 593 and 628 nm (Fig. 6), respectively. The Stokes shift of 123 nm (from 505 to 628 nm) should help to reduce the excitation interference.

As far as we know, two completely different aggregation types, H- and J-aggregation, are involved in the process of formation of nanoparticles. H-aggregates are characterized by blue-shifted absorption bands and fluorescence emission quenching, while J-aggregates tend to induce relatively high fluorescence efficiency with a red-shift of absorption bands [28, 29]. The fluorescence behavior of RAAP

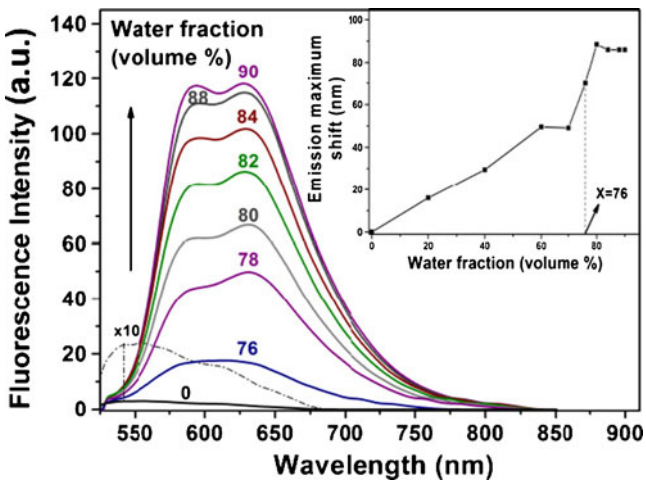

Fig. 6 Fluorescence spectra changes of RAAP (5×10^{-6} M) depending on the volume fraction of water in methanol, λ_{ex}=470 nm. Insert: the change in the emission maximum peak of RAAP

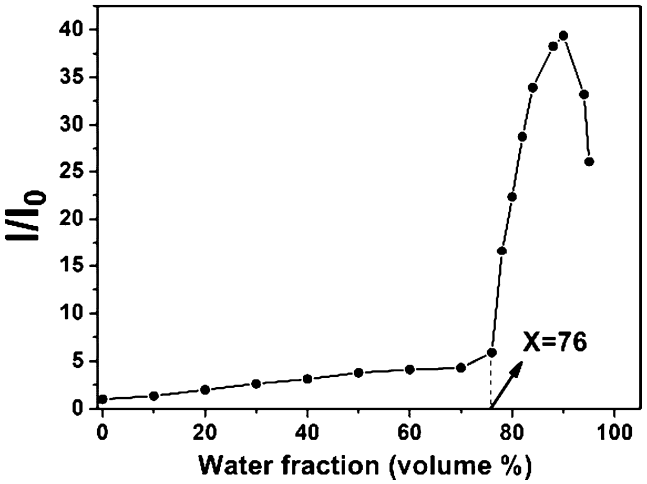

Fig. 7 Variation in the integrated fluorescence intensity of RAAP with the increasing volume fraction of water in methanol

nanoparticles indicates that a J-type aggregation process is carried out. In general, RAAP molecules in isolated state prefer to keep in twisted conformation in dilute solution because of the intramolecular steric interaction between pyrene moiety and rhodanine-3-acetic acid (RAA). It is supposed that the twisted conformation of chromophores in solution tend to suppress the radiative process, whereas, planar ones induced in solid state active the radiative process [5]. From the addition of 76% volume fraction of water, when nanoparticles start to form, effective π-conjugation length of RAAP is extended from isolated twisted molecule to the aggregative planar one. This kind of planarization is attributed to the fact that the intermolecular interaction in solid state is strong enough to overcome intramolecular steric interaction [30, 31]. It is well known that the extended π-conjugation length could do favor for

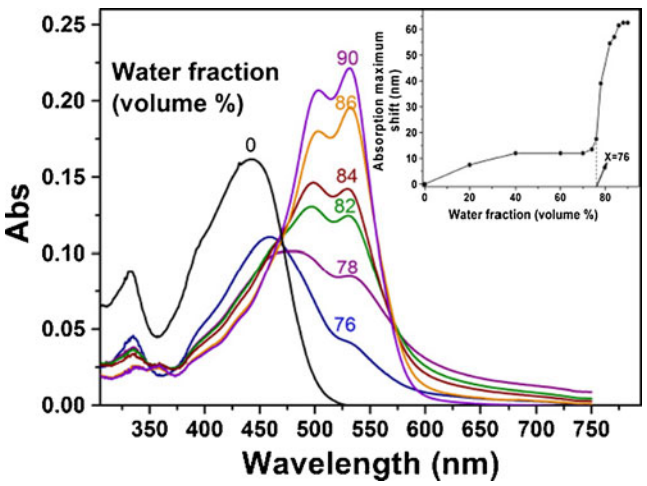

Fig. 8 Absorption spectra changes of RAAP (5×10^{-6} M) depending on the volume fraction of water in methanol. *Insert*: the change of the absorption maximum peak of RAAP

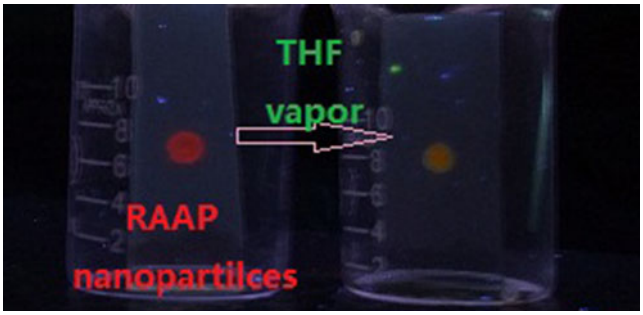

Fig. 9 The fluorescence emission switching behavior of RAAP nanoparticles on TLC plate before (*left*) and after (*right*) the THF vapor is injected under 365 nm irradiation

the formation of π-π stack complex resulting in the fluorescence quenching [32–34]. However, the RAA moiety plays an important role of restricting the parallel face-to-face intermolecular interactions in nanoparticles by its strong steric hindrance and forces RAAP molecules to be arranged in head-to-tail direction to form J-aggregates. Therefore, both the J-aggregation and aggregation-induced intramolecular planarization are considered to be the probable mechanism of strong emission for RAAP nanoparticles.

UV–vis Absorption Properties of RAAP Nanoparticles

The data obtained from absorption spectra of RAAP (5×10^{-6} M) in water/methanol mixtures with different ratios supports our speculation on the mechanism of strong emission in nanoparticle state (Fig. 8). The spectrum of RAAP solution in methanol shows the typical pyrene absorption at 333 nm, along with a low-energy CT band centered at 442 nm [35]. With the addition of water (up to 70%, v/v), the absorption profile is red-shifted slightly ($\Delta\lambda_{max}$=12 nm). After the addition of 76% volume fraction of water, when RAAP nanoparticles starts to form, remarkable spectral changes are observed. The changes are described and explained as below: (1) the decline of pyrene absorption band (333 nm) is sharp and dramatic, indicating that the RAAP molecules are assembled together and the intermolecular interaction is enhanced; (2) the CT band is red-shifted from 440 nm to 502 nm ($\Delta\lambda_{max}$=62 nm), this bathochromic effect implies the extension of effective conjugation length due to the aggregation-induced intramolecular planarization; (3) a new shoulder band centered at 531 nm, which is assigned to J-aggregates of RAAP, is observed and gradually grows to be an intense narrow band after the addition of 76% volume fraction of water. Figure S2 shows the details of absorption spectra. Level-off tails in the visible region, which are due to the Mie scattering effect, are observed after the formation of RAAP nanoparticles [36].

Vapor Experiment

Whereas many dye suspensions in aqueous media gradually bleach of fade with time [26], the nanoparticle solution was very stable. Little, if any, change is detected in the fluorescence and absorption spectra even after keeping it at room temperature without any protection from air and light for more than 3 months. However, the formation of RAAP nanoparticles in water/methanol mixture is found to be reversible when positive solvent, such as methanol and THF, is added. The vapor experiment was undertaken as shown in Fig. 9. RAAP nanoparticles on the TLC plate show bright red emission which turns back to yellow-green in the atmosphere of THF vapor under 365 nm irradiation. The sensing time is about 10 min. Mothanol vapor diaplays the same response. While the negative solvents such as carbon tetrachloride and n-hexane can not lead to this response. The fluorescence emission switching behavior of RAAP nanoparticles indicates its' application in nanosized fluorescence switches which sense organic vapors [5].

Conclusions

In summary, a donor-acceptor compound based on Rhodanineacetic acid-pyrene derivative (RAAP), which emits weak yellow-green fluorescence at 542 nm in methanol solution, was investigated. When the nanoparticles of RAAP are prepared by a simple reprecipitation method, the emission profile is red-shifted to to the red region at 628 nm ($\Delta \lambda_{em}$= 86 nm) and the intensity is 40-fold higher than that in the pure methanol solution. The diameter of nanoparticles is measured to be 50–60 nm by SEM and TEM methods. The red-shift and enhancement of emission spectra are attributed to the synergetic effect of J-aggregation and aggregation-induced intramolecular planarization. We believe that RAAP nanoparticles with remarkable fluorescence efficiency and fluorescence switching behavior will have a number of potential applications in nanosized optoelectronic devices.

Acknowledgments This work was supported at Nanjing University by the Science Foundation of Jiangsu Province (BK2006717) and the State Key Program for Basic Researches of China under Grant Nos. 2009CB929504 and 2007CB936300.

References

1. Empedocles SA, Bawendi MG (1997) Quantum-confined stark effect in single CdSe nanocrystallite quantum dots. Science 278 (5346):2114–2117
2. Alivisatos AP (1996) Semiconductor clusters nanocrystals and quantum dots. Science 271(5251):933–937
3. Hagfeldt A, Gratzel M (1995) Light-induced redox reactions in nanocrystalline systems. Chem Rev 95(1):49–68
4. Schlamp MC, Peng X, Alivisatos AP (1997) Improved efficiencies in light emitting diodes made with CdSe(CdS) core/shell type nanocrystals and a semiconducting polymer. J Appl Phys 82 (11):5837–5842
5. An BK, Kwon SK, Jung SD, Park SY (2002) Enhanced emission and its switching in fluorescent organic nanoparticles. J Am Chem Soc 124(48):14410–14415
6. Kasai H, Kamatani H, Okada S, Nakanishi H et al (1996) Size-dependent colors and luminescences of organic microcrystals. Jpn J Appl Phys 35:L221–L223
7. Kasai H, Kamatani H, Yoshikawa Y, Nakanishi H et al (1997) Crystal size dependence of emission from perylene microcrystals. Chem Lett 26:1181–1182
8. Kasai H, Yoshikawa Y, Seko T, Nakanishi H et al (1997) Optical properties of perylene microcrystals. Mol Cryst Liq Cryst 294:173–175
9. Komai Y, Kasai H, Hirakoso H, Nakanishi H et al (1998) Size and form control of titanylphthalocyanine microcrystals by supercritical fluid crystallization method. Mol Cryst Liq Cryst 322:167–169
10. Yeh HC, Yeh SJ, Chen CT (2003) Readily synthesised arylamino fumaronitrile for non-doped red organic light-emitting diodes. Chem Comm 39:2632–2633
11. Chen CT (2004) Evolution of red organic light-emitting diodes: materials and devices. Chem Mater 16(23):4389–4400
12. Palayangoda SS, Cai XC, Adhikari RM, Neckers DC (2008) Carbazole-based donor−acceptor compounds: highly fluorescent organic nanoparticles. Org Lett 10(2):281–284
13. Chen J, Xu B, Ouyang X, Cao Y et al (2004) Aggregation-induced emission of cis, cis-1,2,3,4-tetraphenylbutadiene from restricted intramolecular rotation. J Phys Chem A 108(37):7522–7524
14. Winnick FM (1993) Photophysics of preassociated pyrenes in aqueous polymer solutions and in other organized media. Chem Rev 93(2):587–614
15. Nishizawa S, Kato A, Teramae N (1999) Fluorescence sensing of anions via intramolecular excimer formation in a pyrophosphate-induced self-assembly of a pyrene-functionalized guanidinium receptor. J Am Chem Soc 121:9463–9464
16. Sahoo D, Narayanaswami V, Kay CM, Ryan RO (2000) Pyrene excimer fluorescence: a spatially sensitive probe to monitor lipid-induced helical rearrangement of apolipophorin III. Biochemistry 39(22):6594–6601
17. Kim JS, Noh KH, Lee SH, Yoon J et al (2003) Molecular Taekwondo. 2. A new calix[4]azacrown bearing two different binding sites as a new fluorescent ionophore. J Org Chem 68(2):597–600
18. Yuasa H, Miyagawa N, Izumi T, Hashimoto H (2004) Hinge sugar as a movable component of an excimer fluorescence sensor. Org Lett 6(9):1489–1492
19. Wang YH, Li B, Zhang LM, Li P et al (2010) A highly selective regenerable optical sensor for detection of mercury(II) ion in water using organic–inorganic hybrid nanomaterials containing pyrene. New J Chem 34:1946–1953
20. Huo C, Chambron JC, Meyer M (2008) Dual emission of a bis (pyrene)-functionalized, perbenzylated β-cyclodextrin. New J Chem 32:1536–1542
21. Xu ZC, Singh NJ, Lim J, Yoon J et al (2009) Unique sandwich stacking of pyrene-adenine-pyrene for selective and ratiometric fluorescent sensing of ATP at physiological pH. J Am Chem Soc 131(42):15528–15533
22. Zhou Y, Kim JW, Yoon J et al (2010) Novel bi-nuclear boron complex with pyrene ligand: red-light emitting as well as electron transporting material in organic light-emitting diodes. Org Lett 12 (6):1272–1275
23. Wu W, Wu W, Ji S, Zhao J et al (2010) Observation of room-temperature deep-red/near-IR phosphorescence of pyrene with cycloplatinated complexes: an experimental and theoretical study. Eur J Inorg Chem 4470–4482

24. Zhang B, Sun J, Yin G, Pu L et al (2011) A highly selective ratiometric fluorescent chemosensor for Ag+ based on a rhodanineacetic acid–pyrene derivative. New J Chem 35:849–853
25. Horn D, Rieger J (2001) Organic nanoparticles in the aqueous phase—theory, experiment, and use. Angew Chem Int Ed 40(23):4330–4361
26. Tong H, Dong Y, Häußler M, Tang BZ et al (2006) Tunable aggregation-induced emission of diphenyldibenzofulvenes. Chem Commun 42(10):1133–1135
27. Upamali KAN, Estrada LA, De PK, Neckers DC et al (2011) Carbazole-based cyano-stilbene highly fluorescent microcrystals. Langmuir 27(5):1573–1580
28. Gruszecki WI (1999) Light-induced excitation quenching and structural transition in light-harvesting complex II. J Biol Phys 59:175–185
29. Birks JB (1970) Photophysics of aromatic moelcules. Wiley, London
30. Baker KN, Farmer AV, Resch T, Farmer BL et al (1993) Crystal structures, phase transitions and energy calculations of poly(*p*-phenylene) oligomers. Polymer 34(8):1571–1587
31. Guha S, Graupner W, Resel R, Leising G et al (1999) Planarity of *para* hexaphenyl. Phys Rev Lett 82(18):3625–3628
32. Tian B, Zerbi G, Müllen K (1991) Electronic and structural properties of polyparaphenylenevinylene from the vibrational spectra. J Chem Phys 95:3198–3207
33. Lagowski JB (2002) Ab initio investigation of conformational and excitation energies of phenylene vinylene oligomers. J Mol Struct 589:125–137
34. Woo HS, Lhost O, Graham SC, Müllen K et al (1993) Optical spectra and excitations in phenylene vinylene oligomers. Synth Met 59(1):13–28
35. Zhou Y, Zhu CY, Gao XS, You XY, Yao C (2010) Hg^{2+}-selective ratiometric and "Off–On" chemosensor based on the azadiene −pyrene derivative. Org Lett 12(11):2566–2569
36. Auweter H, Haberkorn H, Heckmann W, Weiss H et al (1999) Supramolecular structure of precipitated nanosize β-carotene particles. Angew Chem Int Ed 38(15):2188–2191